European Journal of Medicinal Chemistry

DATASET · AUGUST 2015

READS
60

10 AUTHORS, INCLUDING:

Said Bayomi
Mansoura University
50 PUBLICATIONS **188** CITATIONS
SEE PROFILE

Magda El-Sherbeny
Delta University for Science and Technology
29 PUBLICATIONS **398** CITATIONS
SEE PROFILE

Ghada M Suddek
Mansoura University
28 PUBLICATIONS **151** CITATIONS
SEE PROFILE

Shahenda El-Messery
Mansoura University
14 PUBLICATIONS **108** CITATIONS
SEE PROFILE

European Journal of Medicinal Chemistry 101 (2015) 584–594

Contents lists available at ScienceDirect

European Journal of Medicinal Chemistry

journal homepage: http://www.elsevier.com/locate/ejmech

Research paper

Synthesis and biological evaluation of new curcumin analogues as antioxidant and antitumor agents: Molecular modeling study

Said M. Bayomi [a], Hassan A. El-Kashef [b], Mahmoud B. El-Ashmawy [a], Magda N.A. Nasr [c], Magda A. El-Sherbeny [a], Naglaa I. Abdel-Aziz [a], Magda A.-A. El-Sayed [c], Ghada M. Suddek [b], Shahenda M. El-Messery [c], Mariam A. Ghaly [a, *]

[a] Department of Medicinal Chemistry, Faculty of Pharmacy, Mansoura University, Mansoura 35516, Egypt
[b] Department of Pharmacology, Faculty of Pharmacy, Mansoura University, Mansoura 35516, Egypt
[c] Department of Pharmaceutical Organic Chemistry, Faculty of Pharmacy, Mansoura University, Mansoura 35516, Egypt

ARTICLE INFO

Article history:
Received 8 December 2014
Received in revised form
6 July 2015
Accepted 7 July 2015
Available online 14 July 2015

Keywords:
Curcumin analogues
Synthesis
Antioxidant effect
Antitumor effect
Molecular modeling studies

ABSTRACT

New curcumin analogues have been synthesized and their antioxidant activities were investigated by measuring their free radical scavenging capacities. The *in vitro* and *in vivo* antitumor activities of the synthesized compounds on Ehrlich ascites carcinoma (EAC) cell line were evaluated. 4-(4-Chlorophenyl)-2-(5-ethyl-7-(4-methoxybenzylidene)-3-(4-methoxyphenyl)-3,3a,4,5,6,7-hexahydro-2*H*-pyrazolo[4,3-*c*]pyridin-2-yl)thiazole **7h** showed excellent antineoplastic activity in both *in vitro* and *in vivo* studies more than that of tested compounds and reference drug, cisplatin. Different molecular modeling studies were performed, where docking of compound **7h** into telomerase active site suggested that it could exert its antitumor potential by telomerase inhibition.

1. Introduction

Despite significant progress achieved in anticancer therapy, high systemic toxicity and drug resistance remain a major challenge for contemporary medicine in the management of cancers. Chemotherapy causes severe side-effects, which may be due to its cytotoxic effect on normal cells [1]. Therefore, it is important that anticancer drugs display antiproliferative and cytotoxic activity in tumor cells without affecting normal tissues. Reactive oxygen species (ROS) have been linked with cancer, coronary heart disease, and neurodegenerative diseases. Furthermore, their presence in the body causes damage to the DNA of cells. Antioxidants exert their effects by scavenging or preventing the generation of ROS, thus can protect against the formation of free radicals and retard the progress of many chronic diseases, including cancer [1].

Curcumin **(A)** is one of the most potent and multi-targeting phytochemicals against a variety of cancers. The cancer preventive capability of curcumin is linked to its direct antioxidant ability to eliminate free radicals and to reduce oxidative stress [2]. However, the clinical application of curcumin has been significantly limited by its instability and poor metabolic property. A number of synthetic modifications of curcumin have been studied intensively in order to develop a molecule with enhanced bioactivities. A number of curcumin analogues have partial structural resemblance to curcumin motif but are appended with different pharmacophores for targeting proteins that are crucial for survival of tumor cells in question. For example, monocarbonyl 5-carbon spacer, curcumin analogues having cycloalkanone or piperidone central motifs **(B)** were reported to exert good antioxidant and antitumor activities [3,4].

* Corresponding author.
E-mail address: mariamaghaly2@yahoo.com (M.A. Ghaly).

http://dx.doi.org/10.1016/j.ejmech.2015.07.014
0223-5234/

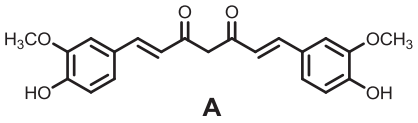

A

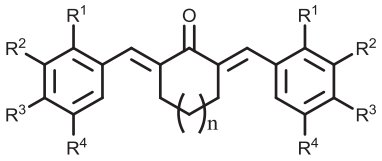

B

Our previous study also showed the incorporation of the shortened carbon linker in heterocyclic parts as hexahydro-2*H*-indazole ring **(C)** and tetrahydro-4*H*-chromene ring **(D)** and reported their promising activities [4].

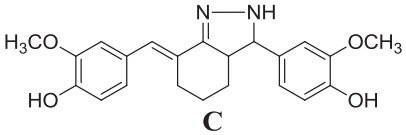

C

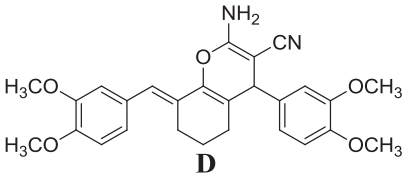

D

Telomere is a non-coding DNA sequence, repeating (5′-TTAGGG-3′), located at the ends of the chromosomes. It functions by preventing chromosomes from losing base pair sequences at their ends. Telomerase, a reverse transcriptase, has been found to be activated in more than 80% of human cancers and, therefore, can be considered as a potential marker for tumorigenesis [5]. Several studies comprising a variety of mechanistic approaches, like mutations and RNA interference of the telomerase enzyme activity, provided the proof of concept for this form of cancer treatment [6–8]. Telomerase provides a good target not only for cancer diagnosis, but also for the development of novel therapeutic agents [9]. Regulation of telomerase activity of cancerous cells by curcumin was estimated and found beneficial to human beings [10,11].

Drug design in the area of cancer therapeutics has used curcumin and its analogues for developing a trend toward more precise mechanisms of cancer cell destruction [12]. So in our research program for novel antitumor agents, we designed and synthesized a series of curcumin analogues based on chalcone scaffold. We chose chalcone moiety as it represents an important pharmacophore of both natural products and synthetic precursors that were found to possess our beseeched biological activity, including antioxidants, and antitumor activities. Recently there is a strong link between curcumin cancer potential and telomerase inhibition [11–18]. So it was quite interesting to make *in silico* study on the most active antitumor curcumin analogue to investigate the mechanistic way for its antiumor potential, and compare it against the least active one.

2. Results and discussion

2.1. Chemistry

The reaction sequences employed for synthesis of the target derivatives are illustrated in Schemes 1–3.

2.1.1. Synthesis of compounds 3 and 4 (Scheme 1)

Thiocarbamoyl pyrazole derivatives **3a,b** were obtained by refluxing equimolar amounts of thiosemicarbazide and the corresponding chalcone **2a,b** in hot ethanolic NaOH solution. The reaction involved nucleophilic attack of the amino group on the polarized carbonyl group, followed by intramolecular cyclization. The spectral and microanalytical data of the formed products were consistent with their structures. The amino functional group was observed at 3280–3463 cm^{-1} in the IR spectra. The evidence for the formation of 4,5-dihydropyrazole ring was obtained from ^{1}H NMR spectrum which provided the diagnostic tool for the positional elucidation of protons. The geminal pyrazoline protons at C4 appeared in the region of 3.20–4.10 ppm as doublet of doublets in all compounds. In addition, CH proton at C5 also appeared as doublet of doublets in the region of 6.10–6.23 ppm due to vicinal coupling with the two non-magnetically equivalent geminal protons of C4. ^{13}C NMR spectrum of compound **3a** confirmed its proposed structure, since the C4 and C5 of pyrazoline ring resonated at 45.11 and 70.20 ppm, respectively. Moreover, the aforementioned compounds **3a,b** were cyclized to pyrazolothiazole derivatives **4a,b** through reaction with phenacyl bromide in ethanol. Analytical and spectral data of the prepared compounds **4a,b** were in agreement with the proposed structure.

2.1.2. Synthesis of compounds 5–8 (Scheme 2)

The key chalcone intermediates **5a–d** were synthesized through condensation of *p*-methoxybenzaldehyde with different cyclic ketones in accordance with the method described in the literature [3]. Heating at reflux equimolar amounts of thiosemicarbazide and the key chalcones **5a–d** in ethanol in the presence of NaOH afforded the corresponding 1-thiocarbamoyl pyrazole derivatives **6a–d**. The thiocarbamoyl moiety in the latter compounds was cyclized to 4-(substituted phenyl)thiazole ring, affording compounds **7a–h** in a good yield. The structures of the new compounds **7a–h** were confirmed using ^{1}H NMR spectra which revealed the presence of 5-H of thiazole in the aromatic region. Moreover, ^{13}C NMR for compound **7c** confirmed the proposed structure due to the appearance of a characteristic peak at δ169.20 corresponding to C_2 of thiazole. In addition, compounds **8a–d** were obtained by the reaction of 1-thiocarbamoyl pyrazole derivative **6b** with chloroacetic acid and different aromatic aldehydes in ethanol. The spectral and microanalytical data of compounds **8a–d** were consistent with their structures. For example, IR spectrum of compound **8a** showed a strong absorption band at 1696 cm^{-1} due to carbonyl group. In addition, ^{13}C NMR confirmed the proposed structure due to the appearance of a signal at 165.11 ppm for the carbonyl group as well as a signal assignable to C2 of thiazole at 160.21 ppm.

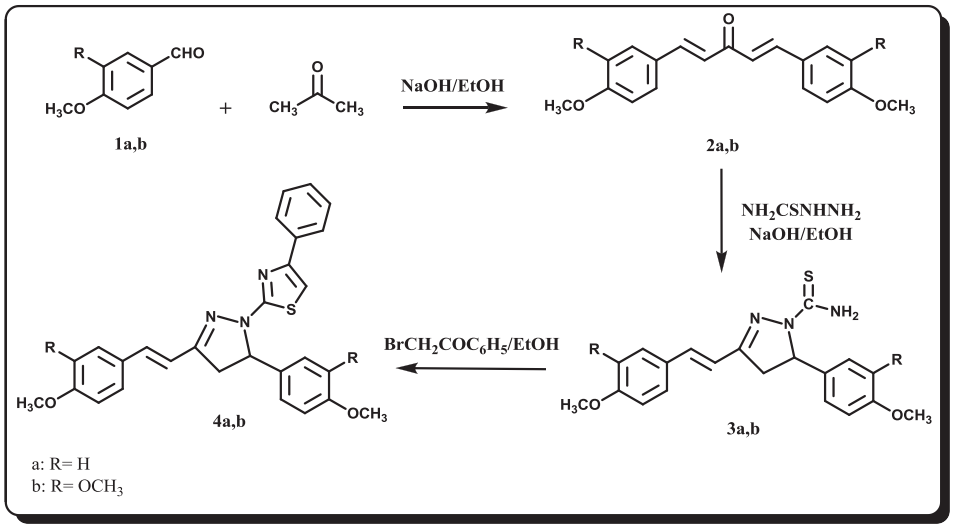

Scheme 1. Synthesis of the designed 1-thiocarbamoyl pyrazole and pyrazolylthiazole derivatives.

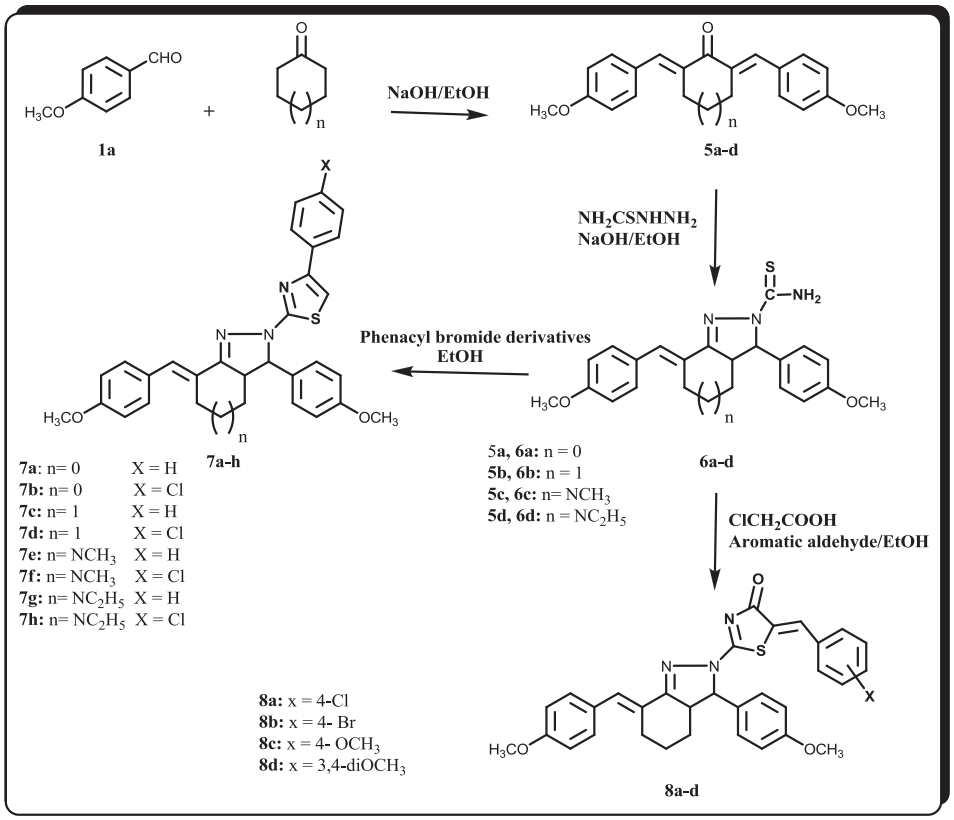

Scheme 2. Synthesis of the designed pyrazolylthiazole and indazolylthiazole derivatives.

2.1.3. Synthesis of compounds 11 (Scheme 3)

Construction of a cyanoaminopyridine ring could be achieved by refluxing a mixture of 2,6-bis(substituted benzylidene)cyclohexanones **10a**–**d** with malononitrile in the presence of ammonium acetate in *n*-butanol to afford the corresponding cyanoaminotetrahydroquinolines **11a**–**d**. The reaction may proceed *via* α,β-unsaturated imino intermediate formed by reaction of ketonic group and ammonium acetate, and stimultaneous Michael addition of malononitrile on α,β-unsaturated moiety to give an adduct, followed by cycloaddition, isomerization, and aromatization to afford 2-amino-3-cyanopyridine derivatives. IR spectra of compounds **11b**–**d** were characterized by the presence of absorption bands assignable to both NH_2 and CN groups in the expected regions of the spectra.

2.2. Biological evaluation

2.2.1. Assay for 2,2′-azino-bis(3-ethylbenzothiazoline-6-sulfonic acid) radical ($ABTS^{\bullet+}$) scavenging activity

The antioxidant activity assay employed here is one of the

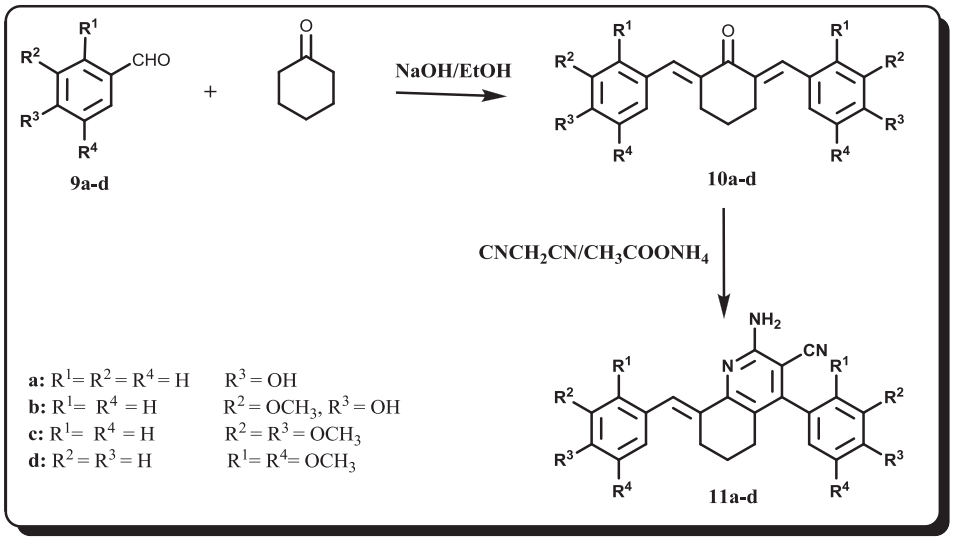

Scheme 3. Synthesis of the designed cyanoaminopyridine derivatives.

several assays that depend on measuring the consumption of stable free radicals, to evaluate the free radical scavenging activity of the investigated compound. The methodology assumes that consumption of the stable free radical ($X^{\bullet}$) by hydrogen-donating antioxidants (YH) will be determined by reaction as follows:

$$X^{\bullet} + YH \rightarrow XH + Y^{\bullet}$$

The rate and/or the extent of the process measured in terms of the decrease in $X^{\bullet}$ concentration, would be related to the ability of the added compounds (YH) to trap free radicals. The decrease in colour intensity of the free radical solution due to scavenging of the free radical by the antioxidant material is measured colourimetrically at a specific wavelength. The assay employs the radical cation derived from 2,2′-azinobis(3-ethylbenzothiazoline-6-sulfonic acid) (ABTS) as stable free radical. The advantage of ABTS–derived free radical method over other methods is that the produced colour remains stable for more than 1 h and the reaction is stoichiometric. In this study, thirteen of the synthesized compounds were subjected to ABTS test and their percentage inhibition of the ABTS radical cation were listed in Table 1. From these results, it is concluded that compounds that exhibited more than 50% inhibition of the ABTS radical cation were in the order of: ascorbic acid > **6d** > **curcumin** > **3a** > **7h** > **4a** > **7f** > **7g** as presented in Fig. 1.

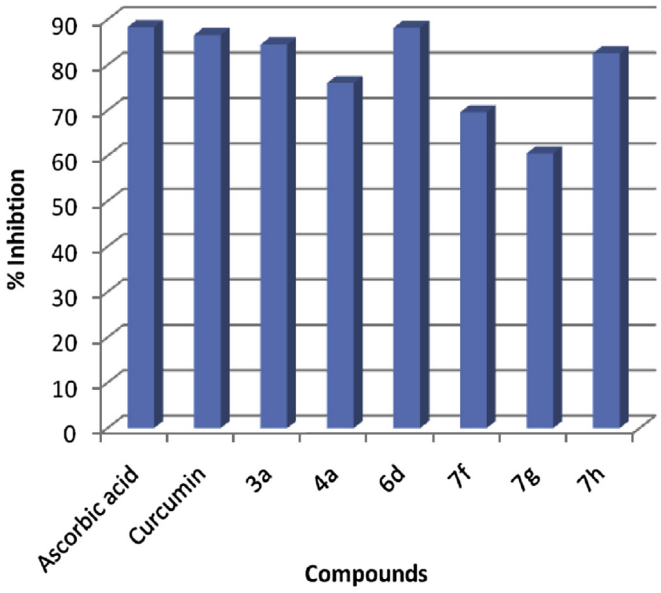

Fig. 1. The percentage inhibition of the ABTS radical cation by the tested compounds.

Table 1
The percentage inhibition of the ABTS radical cation by the tested compounds.

Compound	Absorbance	%Inhibition
Control	0.575	**0**
Ascorbic acid	0.067	**88.34**
Curcumin	0.077	**86.60**
3a	0.089	**84.52**
4a	0.138	**76.00**
6d	0.068	**88.17**
7b	0.417	**27.47**
7f	0.175	**69.56**
7g	0.227	**60.52**
7h	0.100	**82.60**
8a	0.427	**25.73**
8b	0.545	**5.21**
8d	0.465	**19.13**
11a	0.525	**8.69**
11b	0.307	**46.60**
11c	0.519	**9.73**

Compounds **3a** and **6d**, with a thiocarbamoyl substituent at N1 of the pyrazoline ring, showed the highest free radical scavenging activities among the tested compounds with percentage inhibition 84.52 and 88.17, respectively. However, cyclization of the thiocarbamoyl moiety in the latter compounds to a phenylthiazole ring slightly decreased the activity as in compounds **4a**, **7g** and **7h**. The rest of the examined compounds showed weak antioxidant activity except a tetrahydroquinoline derivative, **11b**, that showed percentage inhibition of 46.60.

2.2.2. *Antitumor testing*

This research aimed to evaluate the *in vitro* and *in vivo* antitumor activity of the synthesized compounds on Ehrlich ascites carcinoma (EAC) cell line and this method was proven to give accurate and reliable results as corroborated by the literature [19–21].

2.2.2.1. Antitumor activity using in vitro Ehrlich ascites assay. The antitumor activity of thirteen of the synthesized compounds against EAC cell line was determined using trypan blue assay and cisplatin as a reference drug control. The cells were incubated with three different concentrations (25,50 and100 μM) for each compound and cisplatin. The trypan blue dye exclusion test was used for assessment of cell viability. It is based on the principle that live cells possess intact cell membranes that exclude trypan, whereas dead cells do not and so a viable cell will have a clear cytoplasm and the dead cell will have a blue cytoplasm. Control experiment was also conducted in which EAC cells were incubated in a drug-free medium and the viability of the cells used in control experiments exceeded 95%. Percent survival of cells = (T/C) X 100 was calculated where T and C represent the number of viable cells in a unit volume of the test drug tube and the control tube, respectively (Table 2).

It is evident from the results in Table 2 that the mortality of EAC cells increased with the concentration of the tested compounds as there was an increase in the number of cells stained with trypan blue dye. All the tested compounds showed % dead of cultured EAC cells more than 75% at a concentration of 100 μM in comparison to that of the standard cisplatin (100%). Generally, the most active compounds in this assay were in the order of: **7h** > **11b** > **6d** > **4a** > **7f** > **3a**. Compound **7h** was proved to be the most active member among the tested compound and it appeared promising with antineoplastic activity higher than that of the positive control, cisplatin. Moreover, compound **11b** exhibited equipotent antitumor activity comparable to that of cisplatin.

2.2.2.2. In vivo antitumor study in tumor-bearing mice. To confirm the *in vitro* results, an *in vivo* study was carried out using tumor-bearing mice. Implantation of EAC cells into mice resulted in a solid palpable tumor mass that appeared after 5 days from inoculation (day 0). The size of tumor progressively increased with time and reached about 6-folds its initial mass after additional 21 days (day 21) that considered 100% tumor growth (i.e. 0% tumor growth inhibition). Treatment with cisplatin significantly decreased the relative tumor size compared to the control group, showing 20% tumor growth (i.e. 80% tumor growth inhibition). The synthesized compounds that showed the highest activity in the *in vitro* antitumor assay, **3a**, **4a**, **6d**, **7f**, **7h** and **11b**, were administered to tumour-bearing mice. Antitumor activity was calculated by the determination of ΔT (change of tumor size in the treatment group) and ΔC (change of tumor size in the control). The degree of tumor growth inhibition can be obtained from ΔT/ΔC × 100 (Table 3 and Fig. 2). Compound **7h** showed a promising degree of tumor growth inhibition (82%) being more active than the reference drug cisplatin (80%), while compound **11b** showed equal activity as cisplatin. However, the rest of the screened compounds exhibited reasonable antitumor activities against (EAC) cell line in the following order: **6d** > **3a** > **7f** > **4a** with percentage tumor growth inhibition 77, 76, 70 and 65, respectively.

Table 2
Effect of synthesized compounds on viability of cultured EAC cells *in vitro*.

Compound	% Dead of cultured EAC cells		
	25 μM	50 μM	100 μM
Cisplatin	60	75	100
3a	28.7	57.5	98
4a	30.4	61.6	98.3
6d	31.7	66.5	99
7b	25	47.1	93.5
7f	29.2	58	97.9
7g	27.8	50.2	95.4
7h	98.3	100	100
8a	23.8	46	84
8b	22	43.8	81.6
8d	20.4	40	75.8
11a	21.7	43.4	81
11b	60.2	84	99.7
11c	24.9	45.1	84.2

Table 3
Effect of tested compounds on tumor size in mice after 21 days treatment.

Compound	% Tumor growth inhibition
Control	0
Cisplatin	80
3a	76
4a	65
6d	77
7f	70
7h	82
11b	80

2.3. Molecular modeling studies

2.3.1. Docking study

It was considered interesting to investigate actions of curcumin analogues on signaling molecule antitelomeric activity. The structures of the ligands, the most active compound **7h** and the least active one **8d**, were energy minimized to an RMSD of 0.01 kcal/mol using MMFF94X forcefield. They were docked into telomerase active site and the best and the most energetically favorable conformation of each compound were selected. Minimization methods were used for predicting relative binding affinities of the ligands using energies obtained both in solvent as well as complex phases of each ligand. Molecular docking of the lowest energy conformer (Fig. 3) into ATP binding site of telomerase was performed on the binding model based on the telomerase structure 3DU6 pdb. The binding model of **7h** into telomerase is depicted in (Fig. 4), where it is nicely bound to telomerase with one methoxy group project toward Gln B367, and the methoxy group on the other side forming a more optimal dual interaction, with Lys B169 and Asn B303 through a side chain acceptor binding which might make the 2D structure more stable. These residues influenced the accessibility of the hydrophobic pocket that flanks the active binding site, and their size could be important in controlling telomerase selectivity. Meanwhile, the 2D interaction diagram of the lowest energy conformer of compound **8d** (Fig. 5) showed that the oxygen atom of both methoxy groups didn't show any interactions with any amino acid in telomerase enzyme, and it only shows a single interaction with telomerase through its thiazol-4-one ring (Fig. 6). Hence, This could support the hypothesis that the most active antitumor synthesized compound **7h** could have its both *in vitro* and *in vivo* antitumor activity through telomerase inhibition, in contrary to the least active antitumor synthesized derivative **8d**. Our docking studies provide a good explanation with our preliminary pharmacological experimental data and support further telomerase binding assay methods.

2.3.2. Flexible alignment

Ligand-based active site alignment is a widely adopted technique for the structural analysis of protein–ligand complexes. An alignment is good if a) the strain energy of each molecule is small; b) they have a similar shape; c) their aromatic atoms overlap [22]. Our objective when computing a multiple ligand alignment of a set of input ligands is to maximize the similarity between these ligands, while keeping them in sound conformations. So to probe similarity between the 3D structures of the lowest energy

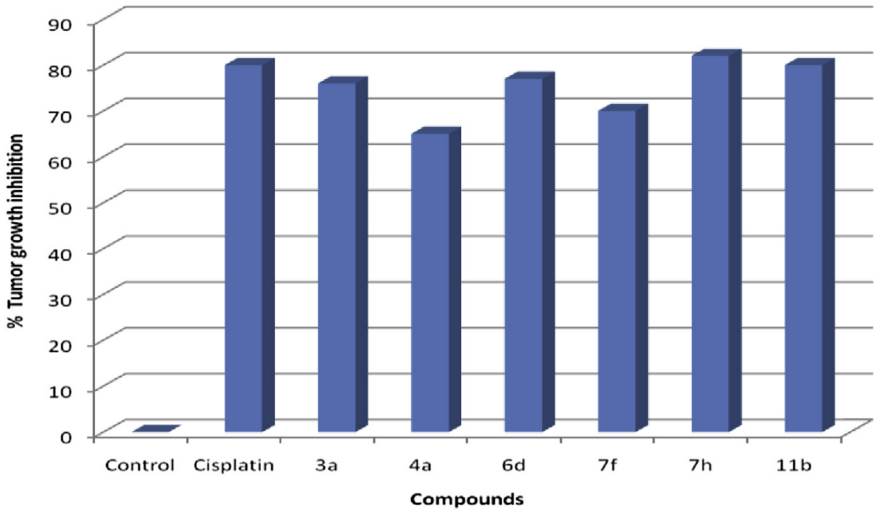

Fig. 2. Percentage tumor growth inhibition by the tested compounds.

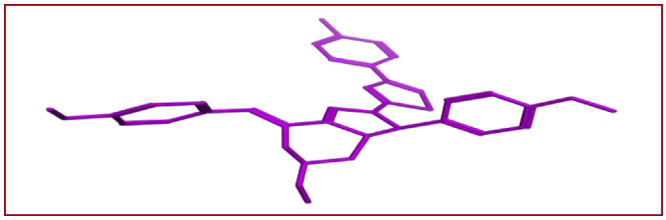

Fig. 3. Lowest energy conformer of most active compound **7h**.

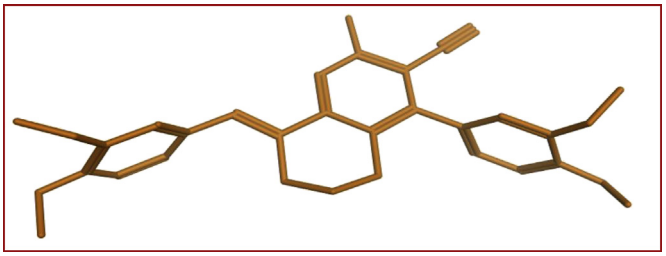

Fig. 5. Lowest energy conformer of least active compound **8d**.

conformers of the most and least active compounds, **7h** and **8d** respectively, flexible alignment was employed. Our initial approach was to employ MOE/MMFF94 flexible alignment to automatically generate superposition of the compounds under investigation with minimal user bias. 200 conformers of each compound were generated and minimized with a distance-dependant dielectric model. A low energy set of 100 was selected for further analysis. The top scoring alignment with the least strain energy is shown in (Fig. 7) where there is a sharp difference in the alignment profile between compound **7h,** and **8d** which is consistent with our experimental data.

2.3.3. *Hydrophopic surface mapping*

In a deep research for reasons behind the diminished activity of compound **8d**, in comparison to the most active one **7h**, hydrophobic surface mapping study was conducted for both compounds in which compound **7h**, pointed out hydrophobic regions (Fig. 8a) **more than** compound **8d** (Fig. 8b). That could be attributed to the cyclic piperidine structure core in addition to the chlorophenyl substitution on the thiazole ring in compound **7h** so it could be deduced that the lipophilicity represents important factor for activity.

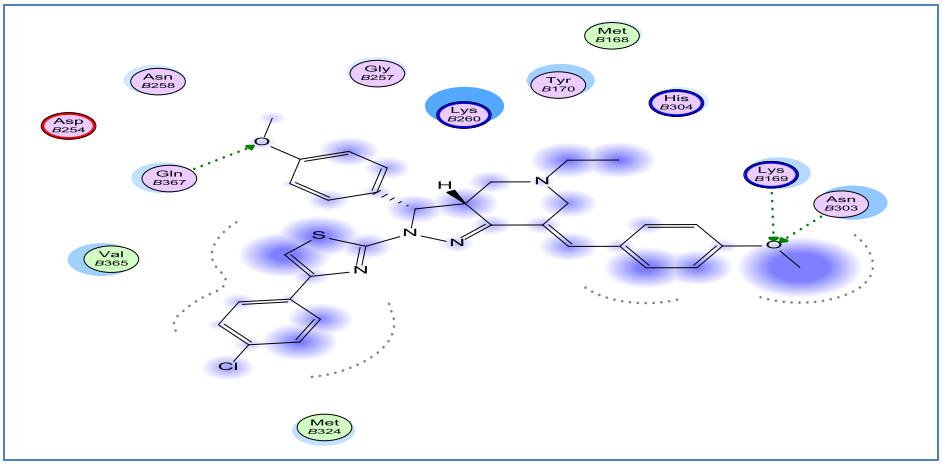

Fig. 4. The 2D binding mode and residues involved in the recognition for compound **7h**, in the telomerase binding pocket.

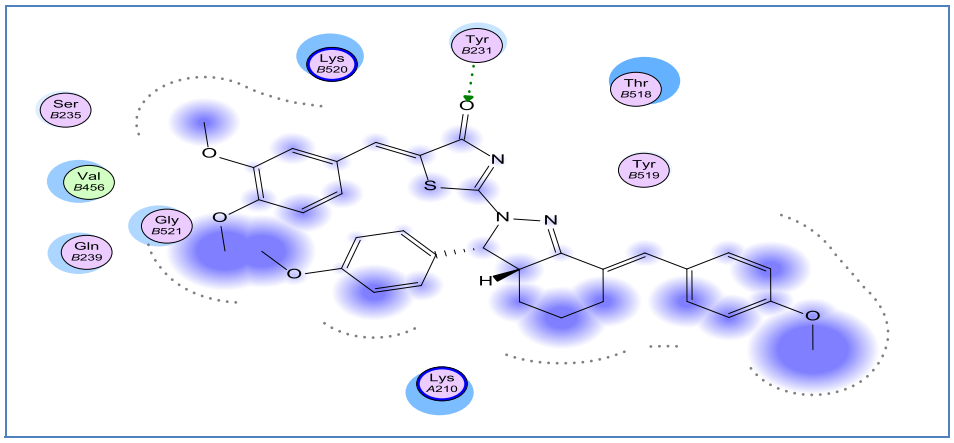

Fig. 6. The 2D binding mode and residues involved in the recognition for compound **8d**, in the telomerase binding pocket.

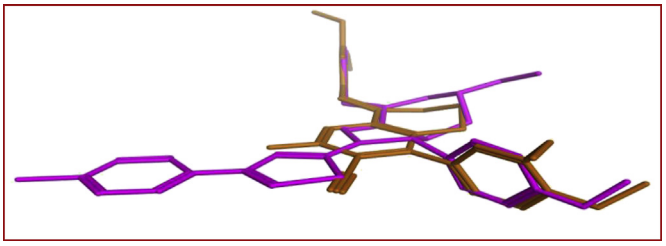

Fig. 7. Flexible alignment of the most active compound **7h** (pink) and the least active compound **8d** (brown). (For interpretation of the references to colour in this figure legend, the reader is referred to the web version of this article.)

3. Conclusion

In this study, a series of chalcone-type newly synthesized curcumin analogues were subjected to antioxidant and antitumor screening. The obtained data revealed that compounds **3a**, **4a**, **6d**, **7f**, **7g**, **7h** and **11b** exhibited significantly higher antioxidant and antitumor activities than other derivatives. Among the latter active compounds, compound **7h** showed excellent *in vitro* and *in vivo* antitumor activities higher than that of cisplatin. In addition, compound **11b** possessed equivalent activity to the standard drug. *In silico* modeling studies were performed. Docking simulation of compound **7h** into the telomerase 3DU6 active site suggested that compound **7h** could exert its antitumor potential by telomerase inhibition. Moreover, conformational analyses, flexible alignment, and hydrophobic mappings of the most active (**7h**) and the least active (**8d**) compounds were applied showing completely different profiles explaining their sharp difference in activity though having similar structure. Modeling studies showed a fairly good agreement with preliminary pharmacological experimental data and support further application of telomerase binding assay methods.

4. Experimental protocols

4.1. Chemistry

Melting points (°C) were recorded using a *Fisher–Johns* melting point apparatus and are uncorrected. Microanalyses were performed in the Microanalytical Unit, Cairo University. IR spectra (KBr) were recorded on Mattson 5000 FT-IR spectrometer (ν in cm^{-1}). ^1H NMR spectra were obtained on FT-NMR spectrometer (200 MHz) Varian Gemini using TMS as internal standard (chemical shifts in ppm, δ units). MS analyses were performed on JEOL JMS-600H spectrometer. Thin layer chromatography (TLC) was performed on silica gel G for TLC (Merck) and spots were visualized by irradiation with ultraviolet light (UV; 254 nm). The syntheses of compounds **2a** [3], **2b** [3], **5a** [3], **5b** [23], **5c** [3], **5d** [3], **10a** [24], **10b** [24], **10c** [25] and **10d** [4] have been previously reported.

4.1.1. General method for the synthesis of 3-(substituted benzylidene)-5-(substituted phenyl)-1-thiocarbamoyl-4,5-dihydro-1H-pyrazole (3a,b)

A mixture of the appropriate chalcone **2a,b** (0.01 mol), thiosemicarbazide (0.9 g, 0.01 mol) and NaOH (1 g, 0.025 mol) in ethanol (50 mL) was refluxed for 8 h. The progress of reaction was monitored by TLC. After the completion of reaction, the reaction mixture was poured into acidic ice water (~pH 2, adjusted by HCl). The separated products was filtered, dried and crystallized from aqueous ethanol.

4.1.1.1. 3-(4-Methoxybenzylidene)-5-(4-methoxyphenyl)-1-thiocarbamoyl-4,5-dihydro-1H-pyrazole (3a). Yield, 40%; mp 135–137 °C; IR (KBr) ν_{max} in cm^{-1} 3440 and 3280 (NH_2), 1579 (C=

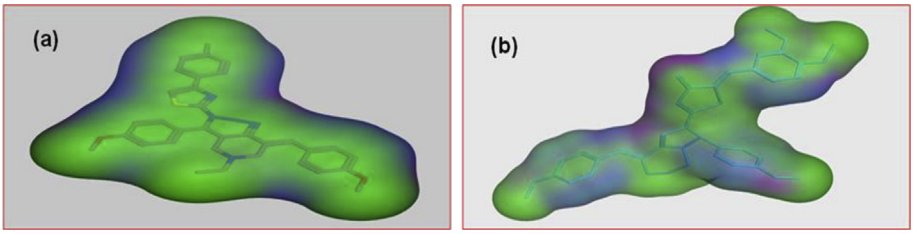

Fig. 8. (a) Surface map for the most active compound **7h** (element) in pocket side. (b) Surface map for the least active compound **8d** (cyan) in pocket side pink: hydrogen bond, blue: mild polar, green: hydrophobic. (For interpretation of the references to colour in this figure legend, the reader is referred to the web version of this article.)

N), 1334 (C=S). ^{1}H NMR ($CDCl_3$); δ 3.20 (dd, J = 5.2, 17,8 Hz, 1H, 4-H of pyrazole), 3.78 (s, 3H, OCH_3), 3.81 (s, 3H, OCH_3), 3.90 (dd, J = 11.9, 17.8 Hz, 1H, 4-H of pyrazole), 6.10 (dd, J = 11.9, 5.2 Hz, 1H, 5-H of pyrazole), 6.71 (br s, 2H, NH_2), 7.10–8.07 (m, 10H, Ar–H and CH=CH). ^{13}C NMR ($CDCl_3$): δ 176.80, 159.21, 159.01, 153.22, 135.11, 134.21, 133.21, 132.11, 129.11, 129.00, 129.23, 115.11, 114.81, 70.21, 54.22, 45.11. Anal. Calcd for $C_{20}H_{21}N_3O_2S$ (%):C, 65.37; H, 5.76; N, 11.44. Found: C, 65.85; H, 6.00; N, 11.94.

4.1.1.2. 3-(4,5-Dimethoxybenzylidene)-5-(4,5-dimethoxyphenyl)-1-thiocarbamoyl-4,5-dihydro-1H-pyrazole (3b). Yield, 50%; mp 121–123 °C; IR (KBr) ν_{max} in cm^{-1} 3463 and 3301 (NH_2), 1577 (C=N), 1336 (C=S).^{1}H NMR ($CDCl_3$); δ 3.34 (dd, J = 5.2, 17.8 Hz, 1H, 4-H of pyrazole), 3.80 (s, 6H, 2OCH_3), 3.88 (s, 6H, 2OCH_3), 4.10 (dd, J = 11.8, 17.2 Hz, 1H, 4-H of pyrazole), 6.23 (dd, J = 11.8, 5.2 Hz, 1H, 5-H of pyrazole), 6.89–8.00 (m, 10H, Ar–H, NH_2 and CH=CH). Anal. Calcd for $C_{22}H_{25}N_3O_4S$ (%):C, 61.81; H, 5.89; N, 9.83. Found: C, 62.10; H, 6.10; N, 10.30.

4.1.2. General method for synthesis of 2-(3-(substituted benzylidene)-5-(substituted phenyl)-4,5-dihydro-1H-pyrazol-1-yl)-4-phenylthiazole (4a,b)

A mixture of compound **3a,b** (0.01 mol), phenacyl bromide (1.9 g, 0.01 mol) in ethanol (50 mL) was heated at reflux for 2 h. After cooling, the separated products was filtered, dried and crystallized from ethanol.

4.1.2.1. 2-(3-(4-Methoxybenzylidene)-5-(4-methoxyphenyl))-4,5-dihydro-1H-pyrazol-1-yl)-4-phenylthiazole (4a). Yield, 45%; mp 155–157 °C; ^{1}H NMR ($CDCl_3$); δ 3.0 (dd, J = 4.5, 18.0 Hz, 1H, 4-H of pyrazole), 3.78 (s, 3H, OCH_3), 3.85 (s, 3H, OCH_3), 3.88 (dd, J = 11.7, 18.0 Hz, 1H, 4-H of pyrazole), 6.0 (dd, J = 11.7, 4.5 Hz, 1H, 5-H of pyrazole), 6.76 (s, 1H, 5-H of thiazole), 7.10–8.27 (m, 15H, Ar–H and CH=CH). ^{13}C NMR ($CDCl_3$): δ 168.10, 159.20, 154.10, 150.20, 135.01, 135.20, 135.11, 130.45, 130.33, 130,25, 130.22, 129.21, 129.11, 128.55, 128.34, 128.00, 127.21, 120.22, 114.22, 114.00, 105.55, 60.22, 55.8, 40.34. Anal. Calcd for $C_{28}H_{25}N_3O_2S$ (%):C, 71.92; H, 5.39; N, 8.99. Found: C, 72.20; H, 5.50; N, 9.20.

4.1.2.2. 2-(3-(4-Dimethoxybenzylidene)-5-(4-dimethoxyphenyl))-4,5-dihydro-1H-pyrazol-1-yl)-4-phenylthiazole (4b). Yield, 60%; mp 145–147 °C; ^{1}H NMR ($CDCl_3$); δ 3.0 (dd, J = 5.2, 18.0 Hz, 1H, 4-H of pyrazole), 3.70 (s, 3H, OCH_3), 3.78 (s, 3H, OCH_3), 3.80 (s, 6H, 2OCH_3), 3.9 (dd, J = 12.0, 18.0 Hz, 1H, 4-H of pyrazole), 6.20 (dd, J = 12.0, 5.4 Hz, 1H, 5-H of pyrazole), 6.80–8.27 (m, 14H, Ar–H, 5-H of thiazole and CH=CH). MS *m/z* (%); 527.00, M^+ (9.14); 55 (100.00). Anal. Calcd for $C_{30}H_{29}N_3O_4S$ (%):C, 68.29; H, 5.54; N, 7.96. Found: C, 68.54; H, 5.90; N, 8,25.

4.1.3. General method for the synthesis of (E)-7(6)-(4-methoxybenzylidene)-3-(4-methoxyphenyl)-2-carbothioamide (6a–d)

A mixture of the appropriate chalcone **5a–d** (0.01 mol), thiosemicarbazide (0.9 g, 0.01 mol) and NaOH (1 g, 0.025 mol) in ethanol (50 mL) was refluxed for 10 h. The progress of reaction was monitored by TLC. After the completion of reaction, the reaction mixture was poured into acidic ice water (~pH 2, adjusted by HCl). The separated product was filtered, dried and crystallized from ethyl acetate.

4.1.3.1. (E)-6-(4-Methoxybenzylidene)-3-(4-methoxyphenyl)-3,3a,4,5,6-pentahydro-2H-cyclopenta[c]pyrazole-2-carbothioamide (6a). Yield, 55%; mp 135–136 °C. ^{1}H NMR ($CDCl_3$); δ 1.30 (m, 2H, CH_2), 1.99–2.27 (m, 3H, CH_2 and CH), 3.80 (s, 3H, OCH_3); 3.82 (s, 3H, OCH_3), 5.52 (d, J = 12.0 Hz, 1H, NCH), 6.55–7.20 (m, 11H, 8ArH, ylidene CH and NH_2, D_2O exchangeable). Anal. Calcd for $C_{22}H_{23}N_3O_2S$ (%): C, 67.15; H, 5.89; N, 10.68. Found: C, 67.55; H, 6.21; N, 10.95.

4.1.3.2. (E)-7-(4-Methoxybenzylidene)-3-(4-methoxyphenyl)-3,3a,4,5,6,7-hexahydro-2H-indazole-2-carbothioamide (6b). Yield, 64%; mp 218–219 °C. IR (KBr) ν_{max} in cm^{-1} 3400 and 3389 (NH_2), 2190 (C≡N), 1672, 1635, 1600 (C=C), and 1291 (C–N).^{1}H NMR ($CDCl_3$); δ 1.30–1.45 (m, 4H, 2CH_2), 1.98–2.26 (m, 3H, CH_2 and CH), 3.70 (s, 3H, OCH_3); 3.75 (s, 3H, OCH_3), 5.32 (d, J = 12.5 Hz, 1H, NCH), 6.45–6.98 (m, 10H, 8ArH and NH_2, D_2O exchangeable), 7.29 (s, 1H, ylidene CH). ^{13}C NMR ($CDCl_3$): δ 174.70, 158.22, 150.22, 134.21, 133.00, 132.50, 132.21, 128.21, 128.11, 127.55, 116.12, 115.54, 71.11, 53.22, 43.21, 26.55, 25.21, 25.00. Anal. Calcd for $C_{23}H_{25}N_3O_2S$ (%): C, 67.79; H, 6.18; N, 10.31. Found: C, 68.10; H, 6.51; N, 10.65.

4.1.3.3. (E)-7-(4-Methoxybenzylidene)-3-(4-methoxyphenyl)-5-methyl-3,3a,4,5,6,7-hexahydro-2H-pyrazolo[4,3-c]pyridine-2-carbothioamide (6c). Yield, 50%; mp 130–131 °C. ^{1}H NMR ($CDCl_3$); δ 2.23 (s, 3H, NCH_3), 2.30–2.45 (m, 3H, NCH_2 and CH), 2.90 (s, 2H, NCH_2), 3.70 (s, 6H, 2OCH_3), 5.32 (d, J = 12.0 Hz, 1H, NCH), 6.55–7.18 (m, 10H, 8ArH and NH_2, D_2O exchangeable), 7.29 (s, 1H, ylidene CH). Anal. Calcd for $C_{23}H_{26}N_4O_2S$ (%): C, 65.38; H, 6.20; N, 13.26. Found: C, 65.90; H, 6.60; N, 13.70.

4.1.3.4. (E)-5-Ethyl-7-(4-methoxybenzylidene)-3-(4-methoxyphenyl)-3,3a,4,5,6,7-hexahydro-2H-pyrazolo[4,3-c]pyridine-2-carbothioamide (6d). Yield, 50%; mp 187–188 °C. ^{1}H NMR ($CDCl_3$); δ 1.03–1.15 (t, 3H, $CH_2\underline{CH_3}$), 2.40–2.50 (m, 3H, NCH_2 and CH), 2.80 (s, 2H, NCH_2), 3.52–3.70 (q, 2H, $\underline{CH_2}CH_3$), 3.80 (s, 6H, 2OCH_3), 5.00 (d, J = 12.1 Hz, 1H, NCH), 6.60–7.30 (m, 11H, 8ArH and NH_2, D_2O exchangeable, ylidene CH). MS *m/z* (%); 436, M^+ (19.63); 437, M^++1 (20.24); 75 (100.00). Anal. Calcd for $C_{24}H_{28}N_4O_2S$ (%): C, 66.03; H, 6.46; N, 12.83. Found: C, 66.43; H, 6.90; N, 13.20.

4.1.4. General method for the synthesis of 2-(pyrazolyl)-4-(substituted phenyl)thiazole derivatives (7a-h)

A mixture of the appropriate 1-thiocarbamoyl pyrazole derivative **6a–d** (0.01 mol) and phenacyl bromide derivative (0.01 mol) in ethanol (50 mL) was heated at reflux for 6 h. The reaction mixture was then evaporated, and the residue obtained was washed with water, collected by filtration, dried, and recrystallized from ethyl acetate to yield the title compounds.

4.1.4.1. (E)-2-(6-(4-Methoxybenzylidene)-3-(4-methoxyphenyl)-3,3a,4,5,6-pentahydrocyclopenta[c]pyrazol-2-yl)-4-phenylthiazole (7a). Yield, 75%; mp 179–180 °C. ^{1}H NMR ($CDCl_3$); δ 1.29 (m, 2H, CH_2), 2.00–2.21 (m, 3H, CH_2 and CH), 3.89 (s, 3H, OCH_3); 3.80 (s, 3H, OCH_3), 5.55 (d, J = 11.5 Hz, 1H, NCH), 6.65–7.79 (m, 15H, 13ArH, ylidene CH and 5-H of thiazole). Anal. Calcd for $C_{30}H_{27}N_3O_2S$ (%): C, 73.00; H, 5.51; N, 8.51. Found: C, 73.50; H, 5.90; N, 9.00.

4.1.4.2. (E)-4-(4-Chlorophenyl)-2-(6-(4-methoxybenzylidene)-3-(4-methoxyphenyl)-3,3a,4,5,6-pentahydrocyclopenta[c]pyrazol-2-yl) thiazole (7b). Yield, 80%; mp 150–151 °C. ^{1}H NMR ($CDCl_3$); δ 1.30 (m, 2H, CH_2), 2.10–2.21 (m, 3H, CH_2 and CH), 3.80 (s, 6H, 2OCH_3), 5.60 (d, J = 11.3 Hz, 1H, NCH), 6.64–7.80 (m, 14H, 12ArH, ylidene CH and 5-H of thiazole). Anal. Calcd for $C_{30}H_{26}ClN_3O_2S$ (%): C, 68.23; H, 4.96; N, 7.96. Found: C, 68.55; H, 5.20; N, 8.50.

4.1.4.3. (E)-2-(7-(4-Methoxybenzylidene)-3-(4-methoxyphenyl)-3,3a,4,5,6,7-hexahydro-2H-indazol-2-yl)-4-phenylthiazole (7c). Yield, 75%; mp 179–180 °C. ^{1}H NMR ($CDCl_3$); δ 1.32–1.46 (m, 4H, 2CH_2), 1.88–2.19 (m, 3H, CH_2 and CH), 3.75 (s, 3H, OCH_3); 3.79 (s, 3H, OCH_3), 5.22 (d, J = 11.0 Hz, 1H, NCH), 6.65–6.78 (m, 15H, 13ArH,

ylidene CH and 5-H of thiazole). ^{13}C NMR ($CDCl_3$): δ 169.20, 158.20, 155.10, 149.50, 136.00, 135.21, 135.01, 129.45, 129.25, 128.25, 128.22, 127.52, 127.11, 126.55, 126.22, 125.20, 125.00, 120.00, 113.22, 112.10, 103.55, 62.32, 51.8, 40.00, 26.21, 24.50, 24.00. Anal. Calcd for $C_{31}H_{29}N_3O_2S$ (%): C, 73.34; H, 5.76; N, 8.28. Found: C, 73.40; H, 5.96; N, 8.60.

4.1.4.4. (E)-4-(4-Chlorophenyl)-2-(7-(4-methoxybenzylidene)-3-(4-methoxyphenyl)-3,3a,4,5,6,7-hexahydro-2H-indazol-2-yl)thiazole (7d). Yield, 83%; mp 169–170 °C. ^{1}H NMR ($CDCl_3$); δ 1.42–1.46 (m, 4H, $2CH_2$), 1.78–2.00 (m, 3H, CH_2 and CH), 3.8 (s, 6H, $2OCH_3$), 5.00 (d, J = 12.0 Hz, 1H, NCH), 6.61–6.77 (m, 14H, 12ArH, ylidene CH and 5-H of thiazole). Anal. Calcd for $C_{31}H_{28}ClN_3O_2S$ (%): C, 68.68; H, 5.21; N, 7.75. Found: C, 69.00; H, 5.60; N, 7.85.

4.1.4.5. (E)-2-(7-(4-Methoxybenzylidene)-3-(4-methoxyphenyl)-5-methyl-3,3a,4,5,6,7-hexahydro-2H-pyrazolo[4,3-c]pyridin-2-yl)-4-phenylthiazole (7e). Yield, 78%; mp 179–180 °C. ^{1}H NMR ($CDCl_3$); δ 2.13 (s, 3H, NCH_3), 2.31–2.44 (m, 3H, NCH_2 and CH), 3.00 (s, 2H, NCH_2), 3.80 (s, 6H, $2OCH_3$), 5.12 (d, J = 11.5 Hz, 1H, NCH), 6.55–7.58 (m, 15H, 13ArH, ylidene CH and 5-H of thiazole). MS *m/z* (%); 522, M^+ (25.37), 85, (100.00). Anal. Calcd for $C_{31}H_{30}N_4O_2S$ (%): C, 71.24; H, 5.79; N, 10.72. Found: C, 71.44; H, 6.11; N, 11.00.

4.1.4.6. (E)-4-(4-Chlorophenyl)-2-(7-(4-methoxybenzylidene)-3-(4-methoxyphenyl)-5-methyl-3,3a,4,5,6,7-hexahydro-2H-pyrazolo[4,3-c]pyridin-2-yl)thiazole (7f). Yield, 80%; mp 170–171 °C. ^{1}H NMR ($CDCl_3$); δ 2.33 (s, 3H, NCH_3), 2.36–2.45 (m, 3H, NCH_2 and CH), 3.10 (s, 2H, NCH_2), 3.88 (s, 6H, $2OCH_3$), 5.14 (d, J = 11.9 Hz, 1H, NCH), 6.45–7.88 (m, 14H, 12ArH, ylidene CH and 5-H of thiazole). Anal. Calcd for $C_{31}H_{29}ClN_4O_2S$ (%): C, 66.83; H, 5.25; N, 10.06. Found: C, 67.05; H, 5.45; N, 10.12.

4.1.4.7. (E)-2-(5-Ethyl-7-(4-methoxybenzylidene)-3-(4-methoxyphenyl)-3,3a,4,5,6,7-hexahydro-2H-pyrazolo[4,3-c]pyridin-2-yl)-4-phenylthiazole (7g). Yield, 80%; mp 220–221 °C. ^{1}H NMR ($CDCl_3$); δ 1.02–1.16 (t, 3H, $CH_2\underline{CH_3}$), 2.30–2.55 (m, 3H, NCH_2 and CH), 2.90 (s, 2H, NCH_2), 3.50–3.80 (q, 2H, $C\underline{H_2}CH_3$), 3.80 (s, 6H, $2OCH_3$), 5.22 (d, J = 12.0 Hz, 1H, NCH), 6.65–7.90 (m, 15H, 13ArH, ylidene CH and 5-H of thiazole). MS *m/z* (%); 536, M^+ (23.17); 537.12, M^++1 (30.00); 75 (100.00). Anal. Calcd for $C_{32}H_{32}N_4O_2S$ (%): C, 71.61; H, 6.01; N, 10.44. Found: C, 71.78; H, 6.50; N, 10.89.

4.1.4.8. (E)-4-(4-Chlorophenyl)-2-(5-ethyl-7-(4-methoxybenzylidene)-3-(4-methoxyphenyl)-3,3a,4,5,6,7-hexahydro-2H-pyrazolo[4,3-c]pyridin-2-yl)thiazole (7h). Yield, 80%; mp 212–213 °C. ^{1}H NMR ($CDCl_3$); δ 1.12–1.17 (t, 3H, $CH_2\underline{CH_3}$), 2.40–2.60 (m, 3H, NCH_2 and CH), 3.00 (s, 2H, NCH_2), 3.40–3.70 (q, 2H, $C\underline{H_2}CH_3$), 3.89 (s, 6H, $2OCH_3$), 6.00 (d, J = 11.0 Hz, 1H, NCH), 6.66–7.80 (m, 14H, 12ArH, ylidene CH and 5-H of thiazole). Anal. Calcd for $C_{32}H_{31}ClN_4O_2S$ (%): C, 67.29; H, 5.47; N, 9.81. Found: C, 67.70; H, 5.40; N, 10.05.

4.1.5. (Z)-5-(4-Substitutedbenzylidene)-2-((E)-7-(4-methoxybenzylidene)-3-(4-methoxyphenyl)-3,3a,4,5,6,7-hexahydro-2H-indazol-2-yl)thiazol-4(5H)-ones (8a–d)

A mixture of the appropriate1-thiocarbamoyl pyrazole derivative **6a–d** (0.01 mol), chloroacetic acid (0.94 gm, 0.01 mol), aromatic aldehyde (0.01 mol) in ethanol (50 mL) was heated at reflux for 16 h. The separated solid was collected by filtration, washed with water, dried and recrystallized from acetonitrile to yield the title compounds.

4.1.5.1. (Z)-5-(4-Chlorobenzylidene)-2-((E)-7-(4-methoxybenzylidene)-3-(4-methoxyphenyl)-3,3a,4,5,6,7-hexahydro-2H-indazol-2-yl)thiazol-4(5H)-one (8a). Yield, 65%; mp 167–168 °C. IR (KBr) ν_{max} in cm^{-1} 1696 (C=O), 2190 (C=N).^{1}H NMR ($CDCl_3$); δ 1.33–1.46 (m, 4H, $2CH_2$), 1.78–2.25 (m, 3H, CH_2 and CH), 3.69 (s, 3H, OCH_3); 3.74 (s, 3H, OCH_3), 5.22 (d, J = 12.0 Hz, 1H, NCH), 6.43–6.99 (m, 14H, 12ArH and 2 ylidene CH). ^{13}C NMR ($CDCl_3$): δ 165.11, 160.21, 158.80, 158.10, 153.11, 135.02, 134.50, 134.23, 134.00, 133.12, 133.00, 130.21, 129.51, 129.41, 127.11, 127.01, 126.20, 126.11, 114.50, 114.20, 114.12, 72.11, 55.8, 40.12, 27.51, 24.23, 24.21. Anal. Calcd for $C_{32}H_{28}ClN_3O_3S$ (%): C, 67.42; H, 4.95; N, 7.37. Found: C, 67.92; H, 5.21; N, 7.00.

4.1.5.2. (Z)-5-(4-Bromobenzylidene)-2-((E)-7-(4-methoxybenzylidene)-3-(4-methoxyphenyl)-3,3a,4,5,6,7-hexahydro-2H-indazol-2-yl)thiazol-4(5H)-one (8b). Yield, 60%; mp 230–231 °C. ^{1}H NMR ($CDCl_3$); δ 1.32–1.46 (m, 4H, $2CH_2$), 1.76–2.26 (m, 3H, CH_2 and CH), 3.90 (s, 6H, $2OCH_3$), 6.00 (d, J = 12.0 Hz, 1H, NCH), 6.55–7.12 (m, 14H, 12ArH and 2 ylidene CH). Anal. Calcd for $C_{32}H_{28}BrN_3O_3S$ (%): C, 62.54; H, 4.59; N, 6.84. Found: C, 63.04; H, 5.11; N, 6.34.

4.1.5.3. (Z)-5-(4-Methoxybenzylidene)-2-((E)-7-(4-methoxybenzylidene)-3-(4-methoxyphenyl)-3,3a,4,5,6,7-hexahydro-2H-indazol-2-yl)thiazol-4(5H)-one (8c). Yield, 70%; mp 199–200 °C. ^{1}H NMR ($CDCl_3$); δ 1.30–1.45 (m, 4H, $2CH_2$), 1.77–2.27 (m, 3H, CH_2 and CH), 3.90 (s, 6H, $2OCH_3$), 3.96 (s, 3H, OCH_3), 5.90 (d, J = 12.2 Hz, 1H, NCH), 6.77–7.40 (m, 14H, 12ArH and 2 ylidene CH). Anal. Calcd for $C_{33}H_{31}N_3O_4S$ (%): C, 70.07; H, 5.52; N, 7.43. Found: C, 70.37; H, 5.42; N, 7.03.

4.1.5.4. (Z)-5-(3,4-Dimethoxybenzylidene)-2-((E)-7-(4-methoxybenzylidene)-3-(4-methoxyphenyl)-3,3a,4,5,6,7-hexahydro-2H-indazol-2-yl)thiazol-4(5H)-one (8d). Yield, 65%; mp 255–256 °C. ^{1}H NMR ($CDCl_3$); δ 1.22–1.37 (m, 4H, $2CH_2$), 1.79–2.27 (m, 3H, CH_2 and CH), 3.91 (s, 6H, $2OCH_3$), 3.97 (s, 6H, $2OCH_3$), 6.00 (d, J = 12.5 Hz, 1H, NCH), 6.87–7.50 (m, 13H, 11ArH and 2 ylidene CH). MS *m/z* (%); 595.50, M^+ (20.10); 596.12, M^++1 (20.00); 151 (100.00).Anal. Calcd for $C_{34}H_{33}N_3O_5S$ (%): C, 68.55; H, 5.58; N, 7.05. Found: C, 68.11; H, 5.28; N, 7.55.

4.1.6. General method for the synthesis of 2-amino-8-(substituted benzylidene)-4-(substituted phenyl)-5,6,7,8-tetrahydroquinoline-3-carbonitriles (11a–d)

A mixture of the appropriate 2,6-bis(substituted benzylidine) cyclohexanone **10a–d** (0.001 mol), malononitrile (0.07 g, 0.001 mol), and ammonium acetate (1.542 g, 0.02 mol) in *n*-butanol (10 mL) was heated under reflux for 10 h. The reaction mixture was concentrated. The separated crystalline solid was collected by filtration, air dried, and recrystallized from ethanol.

4.1.6.1. (E)-2-Amino-8-(4-hydroxybenzylidene)-4-(4-hydroxyphenyl)-5,6,7,8-tetrahydroquinoline-3-carbonitrile (11a). Yield, 50%; mp 250–252 °C. MS *m/z* (%); 369 (M^+, 12.79), 177 (100.00). ^{13}C NMR ($CDCl_3$): δ 161.22, 160.10, 159.23, 157.01, 151.23, 140.11, 131.10, 130.91, 130.21, 129.51, 129.30, 129.01, 123.20, 115.50, 115.11, 114.50, 113.40, 90.12, 35.00, 23.50, 24.30. Anal. Calcd for $C_{23}H_{19}N_3O_2$ (%): C, 74.78; H, 5.18; N, 11.37. Found: C, 75.00; H, 5.48; N, 11.47.

4.1.6.2. (E)-2-Amino-8-(4-hydroxy-3-methoxybenzylidene)-4-(4-hydroxy-3-methoxyphenyl)-5,6,7,8-tetrahydroquinoline-3-carbonitrile (11b). Yield, 50%; mp 247–249 °C. IR (KBr) ν_{max} in cm^{-1} 3416 and 3333 (NH_2), 2202 (C≡N), 1256 (C–N).^{1}H NMR ($CDCl_3$); δ 1.52–2.96 (m, 6H, $3CH_2$), 3.79 (s, 6H, $2OCH_3$), 6.45–6.98 (m, 8H, 6ArH and NH_2, D_2O exchangeable), 7.89 (s, 1H, benzylidene-H), 9.36 (br s, 2H, 2OH, D_2O exchangeable). MS *m/z* (%); 429, M+ (100.00).

Anal. Calcd for $C_{25}H_{23}N_3O_4$ (%): C, 69.92; H, 5.40; N, 9.78. Found: C, 69.40; H, 5.90; N, 10.11.

4.1.6.3. (E)-2-Amino-8-(3,4-dimethoxybenzylidene)-4-(3,4-dimethoxyphenyl)-5,6,7,8-tetrahydroquinoline-3-carbonitrile (11c). Yield, 50%; mp 175–177 °C. IR (KBr) ν_{max} in cm^{-1} 3438 and 3348 (NH_2), 2205 (C≡N), 1253 (C–N).^{1}H NMR ($CDCl_3$); δ 1.59–2.78 (m, 6H, $3CH_2$), 3.78 (s, 12H, $4OCH_3$), 6.49 (s, 2H, NH_2, D_2O exchangeable), 6.84–7.07 (m, 6H, 6ArH), 7.91 (s, 1H, benzylidene-H). MS *m/z* (%); 457, M^+ (0.83), 45 (100.00). Anal. Calcd for $C_{27}H_{27}N_3O_4$ (%):C, 70.88; H, 5.95; N, 9.18. Found: 70.44; H, 5.22; N, 9.00.

4.1.6.4. (E)-2-Amino-8-(2,5-dimethoxybenzylidene)-4-(2,5-dimethoxyphenyl)-5,6,7,8-tetrahydroquinoline-3-carbonitrile (11d). Yield, 50%; mp 48–50 °C. IR (KBr) ν_{max} in cm^{-1} 3438 and 3357 (NH_2), 2209 (C≡N), 1223 (C–N). ^{1}H NMR ($CDCl_3$); δ 1.51–2.97 (m, 6H, $3CH_2$), 3.66 (s, 12H, $4OCH_3$), 5.90 (s, 2H, NH_2, D_2O exchangeable), 6.49–7.08 (m, 6H, 6ArH), 7.85 (s, 1H, benzylidene-H). Anal. Calcd for $C_{27}H_{27}N_3O_4$ (%):C, 70.88; H, 5.95; N, 9.18. Found: C, 71.00; H, 6.00; N, 8.89.

4.2. Biological testing

4.2.1. ABTS test

A mixture of solution of ABTS (2 ml, 0.1 g/100 ml, Sigma–Aldrich, St. Louis, Mo, USA) and solution of MnO_2 (3 ml, 25 mg/ml), prepared in phosphate buffer (pH 7, 0.1 M, BP 1998) was shaken, centrifuged, and decanted. The absorbance (Acontrol) of the resulting green-blue solution (ABTS + radical solution) was recorded at λ_{max} 734 nm. The absorbance (Atest) was measured upon the addition of 20 μl of 1 mg/ml solution of the test sample in spectroscopic grade MeOH/buffer (1:1 v/v) to the ABTS solution. The decrease in absorbance is expressed as % inhibition which is calculated from the equation [26,27].

$$\%\ \text{inhibition} = \frac{A_{control} - A_{test}}{A_{control}} \times 100$$

Ascorbic acid 20 μl (2 mM) solution, and curcumin 20 μl (1 mg/ml) solution were used as standard antioxidants (positive controls). Blank sample was run using solvent without ABTS.

4.2.2. Antitumor testing

EAC cells were established in the Netherlands Cancer Institute. The Ehrlich tumor line was maintained in the laboratory of Faculty of Pharmacy, Mansoura University in female Swiss albino mice by serial intraperitoneal passage at 7–10 day intervals.

4.2.2.1. In vitro cytotoxic assay. Ascitic fluid from the intraperitoneal cavity of the donor animal was aseptically aspirated, 7–8 days after EAC cells inoculation, and washed three times with *N*-2-hydroxyethyl-piperazine-*N*-2-ethanesulfonic acid buffered Hanks' balanced salt solution. EAC cells were counted under the microscope using a haemocytometer and resuspended in normal saline so that each 0.1 ml contained 2×10^5 cells [28]. EAC cells were incubated in RPMI 1640 medium supplemented with 10% fetal calf serum for 24 h in cell culture tubes in a humidified atmosphere containing 5% CO_2 at 37 °C. Each tube contained 0.1 ml cells and 0.9 ml medium (final concentration of the cells = 2×10^5 cells/ml). After 24 h incubation, the tubes were centrifuged at 67 × g and cells were separated. EAC cells were resuspended in RPMI 1640 medium and drugs were added so that the content of each tube was 0.8 ml medium, 0.1 ml cells and 0.1 ml drug. The final concentrations of tested compounds and cisplatin were 25, 50, and 100 μM. After incubation of cells with drugs for 24 h, cells were separated, washed by phosphate buffered saline and resuspended in a drug-free medium. The percent survival of EAC cells was determined by trypan blue dye exclusion method in which the dye stained the dead cells only [29]. Cytotoxicity was determined 3 times and the mean was recorded. Control experiments in which EAC cells were incubated in a drug-free medium were also conducted. Percent survival of cells = (T/C) X 100 was calculated where T and C represent the number of viable cells in a unit volume of the test drug tube and the control tube, respectively.

4.2.2.2. In vivo experiment. Ascitic fluid was withdrawn under aseptic conditions from tumor-bearing mice by needle aspiration from the peritoneal cavity, 7–8 days after EAC cells inoculation, and washed three times with normal saline by centrifugation at 67 × g. EAC cells that obtained after washing were tested for viability using trypan blue. The cells were examined microscopically using a haemocytometer, suspended in normal saline so that each 0.1 ml contained 5×10^5 viable EAC cells. The cells were counted under the microscope. Solid tumors were induced in mice by S.C. inoculation of 0.1 ml containing 5×10^5 viable tumor cells on the left flank anterior to the hind leg. [30] Tumor growth was determined by caliper measurement of the largest diameter and its perpendicular.

$$\text{Tumor size}\left(mm^3\right) = 0.5Xa\ Xb^2.$$

where a is the largest diameter and b is its perpendicular.

When the primary tumor reached a size of 50–100 mm^3, mice were grouped into 14 groups (10 mice each). Group (1) received normal saline (EAC-bearing control, 5 ml/kg). Group (2) received cisplatin (2 mg/kg from 0.1% solution) I.P. Group (3–14) received tested compounds in a dose of 75 mg/kg orally suspended in CMC. Treatment continued for 21 consecutive days. Tumor size at day 0 (five days after tumor inoculation) and after treatment (day 21) was measured. Antitumor activity was calculated by the determination of ΔT (change of tumor size in the treatment group) and ΔC (change of tumor size in the control). The degree of tumor growth inhibition can be obtained from ΔT/ΔC × 100 [31].

4.3. Molecular modeling methodology

4.3.1. Docking study

The three-dimensional structures of compounds **7h** and **8d** which presented best and worst biological profiles, respectively, were constructed using 'Molecular Operating Environment' software (MOE of Chemical Computing Group Inc., 2009.10 on a Core 2 duo 2.3 GHz workstation). Lowest energy conformer of each new analogue 'global-minima' was docked into the telomerase enzyme-binding domain. Starting coordinate of telomerase enzyme, code ID 3DU6, was obtained from the Protein Data Bank of Brookhaven National Laboratory [32]. All the hydrogens were added and enzyme structure was subjected to a refinement protocol in which the constraints on the enzyme were gradually removed and minimized until the RMS gradient was 0.01 kcal/mol A. The energy minimization was carried out using the molecular mechanics force field 'AMBER.' The energy-minimized structure was used for molecular modeling studies keeping all the heavy atoms fixed until a RMSD gradient of 0.05 kcal mol 1 Å1 was reached. Ligand structures were built with MOE and minimized using the MMFF94x forcefield until a RMSD gradient of 0.05 kcal mol 1Å 1 was reached. For both compounds **7h** and **8d**, energy minimizations (EM) were performed using 1000 steps of steepest descent, followed by conjugate gradient minimization to a RMS energy gradient of 0.01 kcal/mol Å [33,34]. The docking was performed using the Alpha Triangle

placement method and the London dG scoring method. 300 results for each ligand were generated, discarding the results with a RMSD value> 3 Å 0.19 The best scored result of the remaining conformations for each ligand was further analyzed. The protein/ligand complexes were minimized using the MMFF94x force field, until an RMSD gradient o 0.1 kcal mol 1 Å 1 was reached.

4.3.2. Flexible alignment

The investigated compounds were subjected to flexible alignment and superposition experiments using the MOE of Chemical Computing Group Inc. software, 2009.10 on Core 2 duo 2.3 GHz workstation. The molecules were built using the Builder module of MOE. Lowest energy aligned conformation(s) were identified. Their geometry was optimized by using the MMFF94 forcefield followed by a flexible alignment using systematic conformational search [35].

Acknowledgment

The authors extend their appreciation to Mansoura University research center, Egypt for funding this work.

References

[1] A. Joseph, C.S. Shah, S.S. Kumar, A.T. Alex, N. Maliyakkal, S. Moorkoth, J.E. Mathew, Synthesis, in vitro anticancer and antioxidant activity of thiadiazole substituted thiazolidin-4-ones, Acta. Pharm. 63 (2013) 397–408.
[2] A.T. Dinkova-Kostova, P. Talalay, Direct and indirect antioxidant properties of inducers of cytoprotective proteins, Mol. Nutr. Food Res. 52 (2008) S128–S138.
[3] K.M. Youssef, M.A. El-Sherbeny, F.S. El-Shafie, H.A. Farag, O.A. Al-Deeb, S.A. Awadalla, Synthesis of curcumin analogues as potential antioxidant, cancer chemopreventive agents, Arch. Pharm. Weinh. 337 (2004) 42–54.
[4] S.M. Bayomi, H.A. El-Kashef, M.B. El-Ashmawy, M.N.A. Nasr, M.A. El-Sherbeny, F.A. Badria, L.A. Abou-zeid, M.A. Ghaly, N.I. Abdel-Aziz, Synthesis and biological evaluation of new curcumin derivatives as antioxidant and antitumor agents, Med. Chem. Res. 22 (2013) 1147–1162.
[5] N. Watanabe, Down regulation of telomerase activity may enhanced by nanoparticle mediated curcumin delivery, Hokkaido Igaku Zasshi 76 (2001) 127–133.
[6] P. Gandellini, M. Folini, R. Bandiera, M. De Cesare, M. Binda, S. Veronese, M.G. Daidone, F. Zunino, N. Zaffaroni, Down-regulation of human telomerase reverse transcriptase through specific activation of RNAi pathway quickly results in cancer cell growth impairment, Biochem. Pharmacol. 73 (2007) 1703–1714.
[7] L. Zou, P. Zhang, C. Luo, Z. Tu, shRNA-targeted hTERT suppress cell proliferation of bladder cancer by inhibiting telomerase activity, Cancer Chemother. Pharmacol. 57 (2006) 328–334.
[8] M. Folini, C. Brambilla, R. Villa, P. Gandellini, S. Vignati, F. Paduano, M.G. Daidone, N. Zaffaroni, Antisense oligonucleotide-mediated inhibition of hTERT, but not hTERC, induces rapid cell growth decline and apoptosis in the absence of telomere shortening in human prostate cancer cells, Eur. J. Cancer 41 (2005) 624–634.
[9] X.D. Gao, Y.R. Chen, Inhibition of telomerase with human telomerase reverse transcriptase antisense enhances tumor necrosis factor-alpha-induced apoptosis in bladder cancer cells, Chin. Med. J. 120 (2007) 755–760.
[10] C. Ramachandran, H.B. Fonseca, P. Jhabvala, E.A. Escalon, S.J. Melnick, Curcumin inhibits telomerase activity through human telomerase reverse transcriptase in MCF-7 breast cancer cell line, Cancer Lett. 184 (2002) 1–6.
[11] N.C.S. Mukherjee, U. Ghosh, N.P. Bhattacharyya, R.K. Bhattacharya, S. Dey, M. Roy, Curcumin-induced apoptosis in human leukemia cell HL-60 is associated with inhibition of telomerase activity, Mol. Cell. Biochem. 297 (2007) 31–39.
[12] J.H. Lee, I.K. Chung, Curcumin inhibits nuclear localization of telomerase by dissociating the Hsp90 co-chaperone p23 from hTERT, Cancer Lett. 290 (2010) 76–86.
[13] Z. Xiao, A. Zhang, J. Lin, Z. Zheng, X. Shi, W. Di, W. Qi, Y. Zhu, G. Zhou, Y. Fang, Telomerase: a target for therapeutic effects of curcumin and a curcumin derivative in Aβ1-42 insult in vitro, PLoS One 9 (2014) e101251.
[14] M. Mollazade, K. Nejati-Koshki, A. Akbarzadeh, N. Zarghami, M. Nasiri, R. Jahanban-Esfahlan, A. Alibakhshi, PAMAM dendrimers augment inhibitory effects of curcumin on cancer cell proliferation: possible inhibition of telomerase, Asian Pac. J. Cancer Prev. 14 (2013) 6925–6928.
[15] M. Nasiri, N. Zarghami, K.N. Koshki, M. Mollazadeh, M.P. Moghaddam, M.R. Yamchi, R.J. Esfahlan, A. Barkhordari, A. Alibakhshi, Curcumin and silibinin inhibit telomerase expression in T47D human breast cancer cells, Asian Pac. J. Cancer Prev. 14 (2013) 3449–3453.
[16] F. Kazemi-Lomedasht, A. Rami, N. Zarghami, Comparison of inhibitory effect of curcumin nanoparticles and free curcumin in human telomerase reverse transcriptase gene expression in breast cancer, Adv. Pharm. Bull. 3 (2013) 127–130.
[17] A.K. Khaw, M.P. Hande, G. Kalthur, Curcumin inhibits telomerase and induces telomere shortening and apoptosis in brain tumour cells, J. Cell. Biochem. 114 (2013) 1257–1270.
[18] I.L. Hsin, G.T. Sheu, H.H. Chen, L.Y. Chiu, H.D. Wang, H.W. Chan, C.P. Hsu, J.L. Ko, N-acetyl cysteine mitigates curcumin-mediated telomerase inhibition through rescuing of Sp1 reduction in A549 cells, Mutat. Res. 688 (2010) 72–77.
[19] M. Gupta, U.K. Mazumder, R.S. Kumar, T. Sivakumar, M.L. Vamsi, Antitumor activity and antioxidant status of *Caesalpinia bonducella* against Ehrlich ascites carcinoma in Swiss albino mice, J. Pharmacol. Sci. 94 (2004) 177–184.
[20] M.E. Zumrutdal, M. Ozaslan, M. Tuzcu, M.E. Kalender, K. Daglioglu, A. Akova, I.D. Karagoz, H. Kilic, O. Colak, F. Koksal, Effect of *Lawsonia inermis* treatment on mice with sarcoma, Afr. J. Biotechnol. 7 (2008) 2781–2786.
[21] N. Bromberg, J.L. Dreyfuss, C.V. Regatieri, M.V. Palladino, N. Duran, H.B. Nader, M. Haun, G.Z. Justo, Growth inhibition and pro-apoptotic activity of violacein in Ehrlich ascites tumor, Chem. Biol. Interact. 186 (2010) 43–52.
[22] P. Labute, C. Williams, M. Feher, E. Sourial, J.M. Schmidt, Flexible alignment of small molecules, J. Med. Chem. 44 (2001) 1483–1490.
[23] L. Wang, J. Sheng, H. Tian, J. Han, Z. Fan, C. Qian, A convenient synthesis of α,α′-bis(substituted benzylidene)cycloalkanones catalyzed by $Yb(OTf)_3$ under solvent-free conditions, Synthesis 18 (2004) 3060–3064.
[24] Z. Du, R. Liu, W. Shao, X. Mao, L. Ma, L. Gu, Z. Huang, A.S.C. Chan, α-Glucosidase inhibition of natural curcuminoids and curcumin analogs, Eur. J. Med. Chem. 41 (2006) 213–218.
[25] N. Singh, J. Pandey, A. Yadav, V. Chaturvedi, S. Bhatnagar, A.N. Gaikwad, S.K. Sinha, A. Kumar, P.K. Shukla, R.P. Tripathi, A facile synthesis of α,α′-(EE)-bis(benzylidene)-cycloalkanones and their antitubercular evaluations, Eur. J. Med. Chem. 44 (2009) 1705–1709.
[26] C.F. Hsu, H. Peng, C. Basle, J. Travas-Sejdic, P.A. Kilmartin, $ABTS^+$ scavenging activity of polypyrrole, polyaniline and poly(3,4-ethylenedioxythiophene), Polym. Int. 60 (2011) 69–77.
[27] E.A. Lissi, B. Modak, R. Torres, J. Escobar, A. Urzua, Total antioxidant potential of resinous exudates from *Heliotropium* species, and a comparison of ABTS and DPPH methods, Free Radi. Res. 30 (1999) 471–477.
[28] O.A. Badary, S.A. Sharaby, S.A. Kenawy, E.E. El-Denshary, F.M. Hamada, Evaluation of cisplatin combined with ondansetron in Ehrlich ascites carcinoma in vitro and in vivo, Tumori 86 (2000) 153–156.
[29] L.M. Weisenthal, P.L. Dill, N.B. Kurnick, M.E. Lippman, Comparison of dye exclusion assays with a clonogenic assay in the determination of drug-induced cytotoxicity, Cancer Res. 43 (1983) 258–264.
[30] R.R.A. Raja, N. Ndupa, D.P. Uma, Effect of macrophage activation on niosome encapsulated bleomycin in tumor-bearing mice, Ind. J. Pharmacol. 28 (1996) 175–180.
[31] M. Schirner, J. Hoffmann, A. Menrad, M.R. Schneider, Antiangiogenic chemotherapeutic agents: characterization in comparison to their tumor growth inhibition in human renal cell carcinoma models, Clin. Cancer Res. 4 (1998) 1331–1336.
[32] A.J. Gillis, A.P. Schuller, E. Skordalakes, Structure of the *Tribolium castaneum* telomerase catalytic subunit TERT, Nature 455 (2008) 633–637.
[33] S. Profeta, N.L. Allinger, Molecular mechanics calculations on aliphatic amines, J. Am. Chem. Soc. 107 (1985) 1907–1918.
[34] N.L. Allinger, Conformational analysis. 130. MM2. A hydrocarbon force field utilizing V_1 and V_2 torsional terms, J. Am. Chem. Soc. 99 (1977) 8127–8134.
[35] S. Kearsley, G.M. Smith, An alternative method for the alignment of molecular structures: maximizing electrostatic and steric overlap, Tetrahedron Comput. Methodol. 3 (1990) 615–633.